Advancing surgical guidance: from (hybrid) molecule to man and beyond

Berg, N.S. van den

CHAPTER 6

MULTIMODAL SURGICAL GUIDANCE DURING SENTINEL NODE BIOPSY FOR MELANOMA: COMBINED GAMMA TRACING AND FLUORESCENCE IMAGING OF THE SENTINEL NODE THROUGH USE OF THE HYBRID TRACER ICG-^{99M}TC-NANOCOLLOID

Adapted from: van den Berg NS, Brouwer OR, Schaafsma BE, Mathéron HM, Klop WMC, Balm AJM, van den Brekel MWM, van Tinteren H, Nieweg OE, van Leeuwen FWB, Valdés Olmos RA. Radiology. 2015:275;530-537.

ABSTRACT

PURPOSE To evaluate the hybrid approach in a large population of patients with melanoma in the head-and-neck, on the trunk, or on an extremity who were scheduled for sentinel node (SN) biopsy.

MATERIALS AND METHODS This prospective study was approved by the institutional review board. Between March 2010 and March 2013, 104 patients with a melanoma, including 48 women (average age: 54.3 years; range 18.5-87.4) and 56 men (average age: 55.2 years; range 22.4-77.4) (p=0.76) were enrolled after obtaining written informed consent.

Following intradermal hybrid tracer administration, lymphoscintigraphy and single photon emission computed tomography combined with computed tomography were performed. Blue dye was intradermally injected prior to the start of the surgical procedure (not in patients with a facial melanoma). Intraoperatively, SNs were initially pursued via gamma tracing followed by fluorescence imaging and, when applicable, blue dye detection. A portable gamma camera was used to confirm SN removal. Collected data included the number and location of the pre- and intraoperatively identified SNs, and the intraoperative number of SNs that were radioactive, fluorescent, and/or blue. A two-sample test for equality of proportions was performed to evaluate differences in intraoperative SN visualization through fluorescence imaging and blue dye detection.

RESULTS Preoperative imaging revealed 2.4 SNs (range 1-6) per patient. Intraoperatively, 93.8% (286 of 305) of the SNs were radioactive, 96.7% (295 of 305) of the SNs were fluorescent, while only 61.7% (116 of 188) of the SNs stained blue ($p<0.0001$). Fluorescence imaging was of value for the identification of near-injection site SNs (two patients), SNs located in complex anatomic areas (head-and-neck (28 patients)), and SNs that failed to accumulate blue dye (19 patients).

CONCLUSION The hybrid tracer enables both preoperative SN mapping and intraoperative SN identification in melanoma patients. In the setup of this study, optical identification of the SNs through the fluorescent signature of the hybrid tracer was superior compared with blue dye-based SN visualization.

INTRODUCTION

Sentinel node (SN) biopsy has evolved into a routine procedure to determine the presence of lymph node metastasis, allowing melanoma patients with nodal metastasis to be treated in a relatively early phase of their disease. Generally, for SN biopsy a combination of technetium-99m (^{99m}Tc)-labeled colloid and blue dye is used. Where radiolabeled colloids enable preoperative SN mapping and intraoperative detection of these particular SNs by using a handheld gamma ray detection probe (hereafter referred to as gamma probe) [1], intraoperative administration of a blue dye can allow the surgeon to optically identify SNs by visualizing their afferent lymphatic vessels. Although successful, this approach has limitations [2]. A deeply located blue lymph vessel may be difficult to find, and its dissection requires substantial expertise. Occasionally, blue dye causes an allergic reaction and it can stain the injection site for months [3,4]. Also, SNs do not always take up blue dye, particularly in the neck. Consequently, the false-negative rate of SN biopsy in melanoma patients is high, 9-21% [5,6].

For radiologically guided SN identification in the preoperative setting, single photon emission computed tomography combined with computed tomography (SPECT/CT) was shown to help place SNs in their anatomic context, enabling better planning of the operation [7-9]. In the surgical suite, the introduction of a portable gamma camera complemented the traditional acoustic guidance provided by the gamma probe [10].

The introduction of near-infrared fluorescence imaging of indocyanine green (ICG) was shown to provide an alternative mode of optical SN identification during the operation [11-16]. Because the near-infrared window lies beyond the visible spectrum, ICG can only be visualized by using a dedicated near-infrared fluorescence camera. Consequently, the use of ICG does not alter the surgical field, nor does it cause tattooing effects of the skin, as does blue dye. However, similar to blue dye, ICG migrates quickly through the lymphatic system, resulting in a limited diagnostic detection window [17]. Although the sensitivity of the signal detection is improved considerably when ICG is used instead of blue dye, the penetration depth of a near-infrared fluorescence dye (<1.0 cm) still prevents preoperative SN mapping.

The hybrid tracer ICG-^{99m}Tc-nanocolloid was developed to combine the attractive migrational properties of a radiolabeled colloid with the favorable optical imaging features of ICG [17,18]. Because of its long-lasting retention in the SNs, a single injection with this hybrid tracer allows preoperative SN mapping and intraoperative radioguided SN identification in a similar fashion as its parental compound ^{99m}Tc-nanocolloid [19]. In addition, it allows fluorescence imaging-based SN visualization of the preoperatively identified SNs. Previously we demonstrated the feasibility of this hybrid approach in various pilot studies [19-25]. In our current study, we evaluated the hybrid approach in a large population of patients with melanoma in the head-and-neck, on the trunk, or on an extremity that were scheduled for SN biopsy.

MATERIALS AND METHODS

PATIENTS

The study protocol was approved by the institutional review board of the Dutch Cancer Institute-Antoni van Leeuwenhoek Hospital (Amsterdam, the Netherlands).

Between March 2010 and March 2013, patients were prospectively included after obtaining written informed consent. Patient inclusion criteria were as follows: (a) age 18 years or older; (b) histologically proven melanoma in the head-and-neck, on the trunk, or on an extremity (Breslow thickness of at least 1.0 mm); (c) no tumor-positive lymph nodes in the regional lymph node basin, as defined by palpation and ultrasonography-guided fine needle aspiration cytology examination; and (d) scheduled for SN biopsy and repeat excision of the melanoma site. Exclusion criteria were as follows: (a) pregnant or breast-feeding woman (in our study no patients were excluded on this basis); (b) patients with a known allergy to iodine (in our study no patients were excluded on this basis); and (c) fluorescence imaging was not performed intraoperatively; because of scheduling logistics, there was no fluorescence camera available in the operating room (in our study 17 patients were excluded on this basis).

Our population consisted of 104 patients, including 48 women (average age: 54.3 years, range 18.5-87.4) and 56 men (average age: 55.2 years; range 22.4-77.4) (p=0.76), with an average Breslow thickness of 2.7 mm (range 1.0-10.0 mm). The first 13 patients were also included in previous feasibility trials [19,21].

TRACER PREPARATION

ICG-^{99m}Tc-nanocolloid (size 10-100 nm) was prepared via non-covalent self-assembly of ^{99m}Tc-labeled nanocolloid (GE Healthcare, Eindhoven, the Netherlands) and ICG (Pulsion Medical Systems, Munich, Germany), as previously described [20].

^{99m}Tc-nanocolloid is approved for lymphatic mapping by the European Medicines Agency, and ICG is used off-label for this application but is U.S. Food and Drug Administration approved for intravenous use (up to 2.0 mg/kg body weight). In the ICG-^{99m}Tc-nanocolloid complex, the ratio of ICG to human serum albumin is 18:1 [26]. While the amount of ^{99m}Tc-nanocolloid is identical to that used for radioguided SN biopsy [19], the dose of ICG used (<0.05 mg) is substantially lower than the amount of ICG allowed for intravenous use.

PREOPERATIVE PROCEDURE

Operating room logistics aided in determining whether the patient was injected with the hybrid tracer on the day before, or on the morning of, the operation. An average of 78.5 MBq (range 57.4-112.9 MBq) of ICG-^{99m}Tc-nanocolloid was intradermally injected around the melanoma site (four deposits; total volume, 0.4 mL). This variability is tracer-decay-dependent and was influenced by the time the volume for injection was extracted from the vial.

To visualize the draining lymphatic vessels and the first draining lymph nodes, during the first 10 min after injection, anterior and lateral dynamic lymphoscintigraphy was performed by using a dual-head gamma camera (Symbia T; Siemens, Erlangen, Germany). This step was followed by acquisition of static planar lymphoscintigrams at 15 min after injection. At 2 h after injection, again static planar lymphoscintigrams were obtained, followed by SPECT and low-dose CT (40 mAs, 130 kV) (Symbia T; Siemens) acquisitions. After correction for scatter and tissue attenuation, SPECT and CT images were fused. Multiplanar reconstruction enabled comparison of fused SPECT/CT images with concomitant CT images (Osirix medical imaging software; Pixmeo, Geneva, Switzerland). One author (R.A.V.O., with 21 years of experience with SN biopsy for melanoma) and three other nuclear medicine physicians who are not authors of our study (with 7, 10, and 14 years of experience with SN biopsy) evaluated the acquired imaging data for the number of SNs visualized, and the basin in which the SN was located. Lymph nodes on a direct drainage pathway from the site of injection were classified as SNs (hereafter referred to as preoperative SNs) [27,28].

SURGICAL PROCEDURE

Before the start of the operation, 1.0 mL of blue dye V (Laboratoire Guerbet, Aulnay-Sous-Bois, France) was injected intradermally around the melanoma site (circular injection) in the patients with melanoma located outside the facial area (n=69). Operations were performed by three authors (W.M.C.K., A.J.M.B., O.E.N., with 7, 7, and 21 years of experience with SN biopsy for melanoma, respectively) and others who are not authors of our study.

Generally, SN biopsy was performed before excision of the melanoma site. However, in 44 patients with a head-and-neck melanoma, the surgeon removed the melanoma site prior to performing SN biopsy; here, the surgeon reasoned that leaving the melanoma site in situ would affect radioactivity-based SN identification because of the high background signal coming from the injected melanoma site.

Preceding the start of SN biopsy, an overview image of the radioactive hot spots was acquired by using a portable gamma camera (Sentinella; Oncovision, Valencia, Spain) [10]. Preoperative SNs were initially pursued with the gamma probe (Neoprobe; Johnson & Johnson Medical, Hamburg, Germany), and when possible, attempts were made to visualize the tumor draining lymphatic vessels via blue dye. Alternating attempts were then made to optically visualize the preoperative SN through fluorescence imaging by using a handheld near-infrared fluorescence camera (PhotoDynamic Eye; Hamamatsu Photonics K.K., Hamamatsu, Japan) and, when applicable, visual detection of blue dye. Fluorescence imaging required the lights in the operating room to be dimmed to minimize the background signal.

To verify complete preoperative SN removal, after excision of the preoperative SNs, another portable gamma camera image was acquired. If residual radioactivity was

observed at the site of a previously excised SN, the node was considered part of a cluster of multiple adjacent SNs. Since it is not possible to discriminate between nodes in a cluster, these nodes were considered to be additional intraoperative SNs and also were harvested using the above described combination. In case of clustered nodes, after the operation, the acquired SPECT and CT images were retrospectively evaluated for visibility of these clusters on the images by three authors (R.A.V.O., O.R.B., N.S.v.d.B., with 21, 5, and 3 years of experience, respectively).

Prior to closing, the wound area was evaluated for non-radioactive non-fluorescent but blue nodes and palpated for enlarged lymph nodes suspicious for metastasis that were not radioactive, fluorescent, or blue.

Intraoperatively, SNs were classified for being radioactive (yes or no), fluorescent (yes/no), or blue (yes/no) by the surgeon (W.M.C.K., A.J.M.B., O.E.N., and others who are not authors of our study. The data were collected by a clinical researcher (N.S.v.d.B., O.R.B., B.E.S., H.M.M., with 3 years, 5 years, 3 years, and 1 year of experience with image-guided SN biopsy, respectively).

HISTOPATHOLOGY AND EX VIVO ANALYSES

Excised SNs were formalin fixed, bisected, and paraffin embedded, and they were cut at a minimum of six levels at 50-150 µm intervals. Histopathological evaluation was performed by a pathologist (3-20 years of experience) and included staining (hematoxylin and eosin (S-100, catalog no. Z0311; Dako, Heverlee, Belgium) and MART-1 (catalog no. M7196; Dako)).

STATISTICAL ANALYSIS

A two-sample test for equality of proportions with continuity correction (R version 3.0.2; www.r-project.org) was performed to evaluate the difference in average age between male and female patients and to evaluate differences in the number of fluorescent and blue nodes in the overall population and for each subgroup. A p-value <0.05 was considered to indicate a significant difference.

RESULTS

PREOPERATIVE RESULTS

A total of 246 SNs were preoperatively identified in 104 patients (average 2.4 preoperative SNs per patient; range 1-6; Table 1). A SPECT/CT scan was acquired in all patients, and in all but one patient, this scan provided useful anatomic landmarks that facilitated virtual planning of the surgical procedure. In the remaining patient, the portable gamma camera was used to locate a pre-auricular SN close to the injection site that was not seen on the acquired lymphoscintigrams or on the SPECT/ CT images.

Table 1. Preoperative sentinel node mapping results

	Overall			
Primary melanoma location		***Head-and-Neck***	***Trunk***	***Extremity***
# Patients	104	53	33	18
Total # SNs visualized (av; range)	246 (2.4; 1-6)	137 (2.6; 1-6)	76 (2.3; 1-4)	33 (1.8; 1-3)
- Lymphoscintigraphy (% total)	232/246 (94.3%)	127/137 (92.7%)	73/76 (96.1%)	32/33 (97.0%)
- SPECT/CT (% total)	245/246 (99.6%)	136/137 (99.3%)	76/76 (100.0%)	33/33 (100.0%)
- Portable gamma camera (% total)	1/246 (0.4%)	1/137 (0.7%)	-	-
Total # basins in which SNs were visualized (av; range)	183 (1.8; 1-6)	111 (2.1; 1-5)	53 (1.6; 1-4)	19 (1.1; 1-2)
Distribution of SNs visualized according to basins				
- Suboccipital	8/183 (4.4%)	8/111 (7.2%)	-	-
- Temporal	1/183 (0.5%)	1/111 (0.9%)	-	-
- Parotid gland	8/183 (4.4%)	8/111 (7.2%	-	-
- Retro- or pre-auricular	18/183 (9.8%)	18/111 (16.2%)	-	-
- Neck	75/183 (41.0%)	74/111 (66.7%)	1/53 (1.9%)	-
- Supraclavicular	4/183 (2.2%)	2/111 (1.8%)	2/53 (3.8%)	-
- Scapular	2/183 (1.1%)	-	2/53 (3.8%)	-
- Pectoral	1/183 (1.1%)	-	1/53 (1.9%)	-
- Epitrochlear	1/183 (1.1%)	-	-	1/19 (5.3%)
- Axilla	44/183 (24.0%)	-	40/53 (75.5%)	4/19 (21.1%)
- Intermediate trunk	1/183 (0.5%)	-	1/53 (1.9%)	-
- Groin	20/183 (10.9%)	-	6/53 (11.3%)	14/19 (73.7%)

= number; SPECT/CT = single photon emission computed tomography combined with computed tomography; SN = sentinel node; av = average.

INTRAOPERATIVE RESULTS

In the one-day protocol, the surgical procedure started, on average, 5 h after injection (range 3-10 h after injection; 58 patients). In the two-day protocol, the procedure started approximately 21 h after injection (range 18-27 hours after injection; 46 patients).

All but four preoperatively identified SNs could be intraoperatively localized through the combined use of gamma tracing, fluorescence imaging, or blue dye guidance. In 33 patients, 59 additional SNs (intraoperatively identified SNs) were excised on the basis of the combination of gamma detection and fluorescence imaging. Re-analysis of the respective CT images revealed the presence of clustered nodes located at the location of a single hot spot on the corresponding SPECT images (Figures SI1-3). Intraoperatively, in total, 301 SNs were harvested (average 2.9 SNs per patient; range, 1-9(; (Table 2).

Table 2. Intraoperative sentinel node detection

	Overall (104 patients	***No blue dye used (35 patients)***	***Blue dye used (69 patients)***						
			Injection site first (13 patients)	***Sentinel node biopsy first (56 patients)***					
									Total
Basin		***Head-and-Neck[±]***	***Other[@]***	***Head-and-Neck[±]***	***Head-and-Neck[±]***	***Axilla***	***Groin***	***Aberrant[%]***	***Other[@]***	
# Excised SNs	301	112	2	49	18	72	38	6	4	138
# Not-excised SNs	4	3	-	-	-	1	-	-	-	1
Total	305	115	2	49	18	73	38	6	4	139
Intraoperative SN detection										
- With gamma tracing	286/305 (93.8%)	102/115 (88.6%)	2/2 (100.0%)	46/49 (93.9%)	17/18 (94.4%)	71/73 (97.3%)	38/38 (100.0%)	6/6 (100.0%)	4/4 (100.0%)	136/139 (97.8%)
- With fluorescence guidance	295/305 (96.7%)	111/115 (96.5%)	2/2 (100.0%)	49/49 (100.0%)	16/18 (88.9%)	69/73 (94.5%)	38/38 (100.0%)	6/6 (100.0%)	4/4 (100.0%)	133/139 (95.7%)
- With blue dye visualization	116/188 (61.7%)	-	-	19/49 (38.8%)	4/18 (22.2%)	54/73 (74.0%)	35/38 (92.1%)	2/6 (33.3%)	2/2 (50.0%)	97/139 (69.8%)
p-value[$]	p<0.0001	-	-	p<0.0001	p=0.0002	p=0.0008	p=0.24	p=0.14	p=0.41	p<0.0001

[±] head-and-neck includes subocciptial, temporal, retro- and pre-auricular basins, the parotid gland, and the neck basins. [@] Other includes supraclavicular and epitrochlear basins. [%] Abberant includes intermediate trunk, pectoral, and scapular basins. [$] Two-sample test for equality of proportions with continuity correction between detection by fluorescence imaging and visual blue dye detection. # = number; pts = patients; SN = sentinel node.

In the overall population, 93.8% (286 of 305) of the excised SNs could be intraoperatively localized with gamma tracing by using the gamma probe. Optical identification of the SNs with fluorescence imaging identified 96.7% (295 of 305) of the nodes, while only 61.7% (116 of 188) of the SNs had stained blue at the time of excision ($p<0.0001$; Table 2). Intraoperatively, no SNs were found that were solely blue.

To allow continuous drainage after the intraoperative injection of blue dye, SN biopsy is ideally performed before repeat excision of the melanoma site. Looking more closely at this specific subset of patients (Table 2, "Blue dye used" columns, "SNB first" column, "Total" column), merely 69.8% (97 of 139) of the SNs were blue at the time of excision, whereas fluorescence imaging allowed visualization of 95.7% (133 of 139) of the SNs ($p<0.0001$).

In 23 patients with drainage to the head-and-neck and two patients with drainage to the groin, fluorescence imaging allowed the surgeon to determine the exact location of the preoperative SNs. Fluorescence imaging was used by the surgeon to pinpoint the preoperative SNs with a forceps in eight of these 25 patients. In five of these patients, preoperative SNs were already visualized transcutaneously (Figure 1), allowing the surgeon to determine the site of incision.

In five patients, fluorescence imaging aided in the localization of the preoperative SN as radioactivity-based detection of the preoperative SNs was not possible because of the high background signal coming from the nearby injection site. In four of these five patients, the preoperative SN was located in the parotid gland (melanoma site, temporal bone (n=3) or preauricular area (n=1)) and in the other patient, the preoperative SN was located in level III (melanoma site, cheek).

Fluorescence imaging confirmed gamma probe-based localization of the preoperative SNs when no blue dye was used (n=3 patients) but also allowed for optical identification of preoperative SNs that failed to take up blue dye (n=19 patients; Figures 2, 3). In three patients, through fluorescence imaging the lymphatic duct running to the preoperative SN could be visualized (Figures 3, 4).

Pathologic analysis of the excised nodes revealed 36 SN metastases in 25 patients. Nodal involvement was found in 15.1% (eight of 53), 33.3% (11 of 33), and 33.3% (six of 18) of patients with head-and-neck melanoma, melanoma of the trunk, or on an extremity, respectively. In five patients with a melanoma on the trunk, aberrant drainage was seen. In two of these five patients, the aberrantly located SN was the only tumor-positive node.

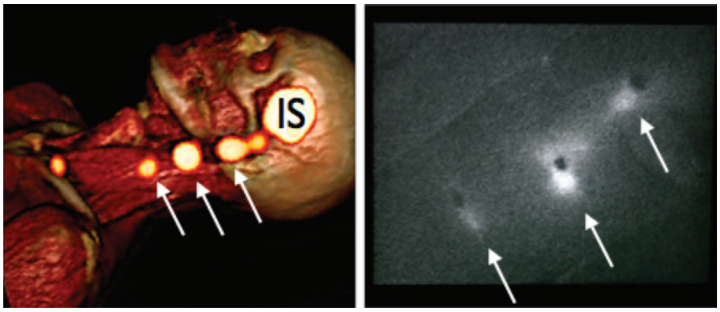

Figure 1. Transcutaneous sentinel node identification through fluorescence imaging in a 70-year-old female with melanoma on the head (temporal left; Breslow thickness 2.0 mm). The patient was scheduled for re-excision of the melanoma scar and subsequent SN biopsy. Due to the location of the melanoma, no blue dye was injected intraoperatively. Left) 3D SPECT/CT-based volume rendering after cropping of the skin. The image shows three SNs (white arrows); Right) Intraoperative fluorescence imaging visualized the temporal, pre-auricular and level II SN already transcutaneously. SN = sentinel node; SPECT/CT = single photon emission computed tomography combined with computed tomography.

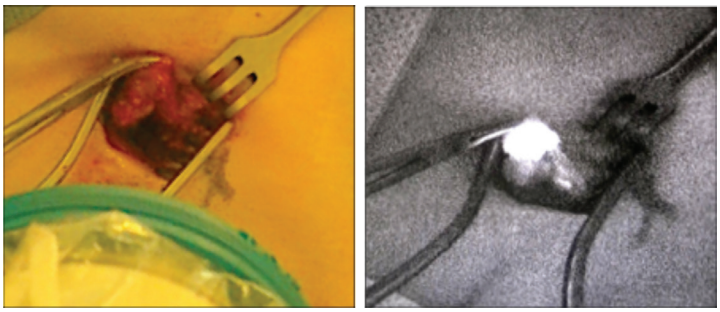

Figure 2. Optical sentinel node identification via fluorescence imaging in a 25-year-old female with a melanoma of the trunk (on the back, paramedian; Breslow thickness 1.1 mm). The patient was scheduled for re-excision of the melanoma scar and subsequent SN biopsy. Preoperatively two SNs were visualized (left and right axilla). Directly before the start of the operation 1.0 mL blue dye was injected. Left) Axillary tissue harbouring the SN; Right) Fluorescence imaging-based identification of the SN which did not stain blue. SN = sentinel node.

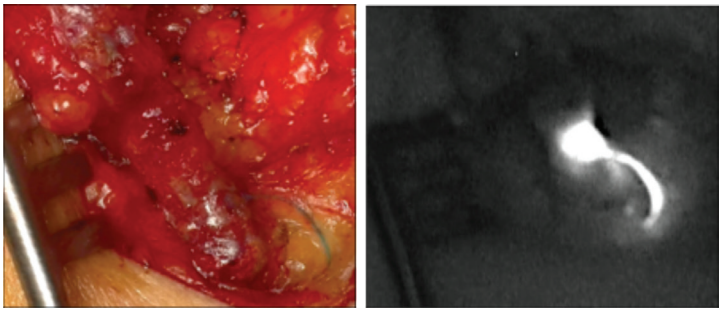

Figure 3. Optical sentinel node identification vial fluorescence imaging in a 20-year-old female with a melanoma of the trunk (abodomen, paramedian right; Breslow thickness 1.1 mm). The patient was scheduled for re-excision of the melanoma scar and subsequent SN biopsy. Preoperatively three SNs were visualizd (right and left groin and in the right axilla). Directly before the start of the operation 1.0 mL blue dye was injection. Left) Identification of a blue afferent lymphatic duct running to a SN in the left groin; Right) Fluorescence imaging-based identification of the SN and its afferent lymphatic duct. SN = sentinel node.

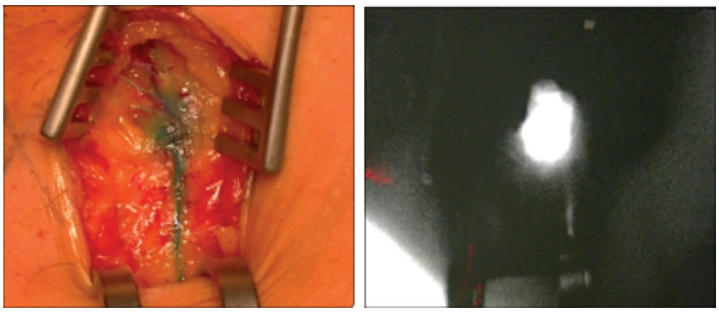

Figure 4. Optical sentinel node identification in a 51-year-old female patient with a melanoma of an extremity (left upper leg; Breslow thickness 2.0 mm). The patient was scheduled for re-excision of the melanoma scar and subsequent SN biopsy. Preoperatively a SN was visualized in the left groin. Directly before the start of the operation 1.0 mL blue dye was injected. Left) Clear blue dye-based visualization of the afferent lymphatic duct running to the blue stained SN; Right) Fluorescence imaging-based visualization of the same SN and its afferent lymphatic duct. SN = sentinel node.

DISCUSSION

Our study in 104 patients with melanoma confirms what previous feasibility studies suggested, namely that the hybrid approach, making use of ICG-^{99m}Tc-nanocolloid, provides improved intraoperative guidance toward preoperative SNs; with additional fluorescence imaging during surgery, 35.1% more SNs could be optically visualized than with blue dye (in the group of patients in which blue dye was used, fluorescence imaging allowed visualization of 182 of 188 SNs (96.8%), whereas with blue dye, 116 of 188 SNs (61.7%) were visualized).

Overall, the percentage of SNs that could be identified during the operation by using gamma tracing and fluorescence imaging was comparable (93.8% (286 of 305) and 96.7% (295 of 305), respectively). The finding that SNs were more often fluorescent than blue (96.7% (295 of 305) vs. 61.7% (116 of 188), respectively; $p<0.0001$) may imply a superior optical identification rate for the hybrid tracer in comparison with conventional blue dye. This advantage was most pronounced in patients with drainage to the head-and-neck.

In our study, we did not solely rely on intraoperative fluorescence imaging to identify the preoperative SNs; rather, the hybrid approach was taken in which preoperative images provided a roadmap for initial surgical exploration. Results of recent studies with the use of 'free' ICG further underline the value of preoperative imaging by stating that in-depth SN identification provided by radiolabeled colloids is superior to that provided by ICG [13,14]. Namikawa et al. [14] showed that, especially in patients with axillary SNs or patients with a high body mass index, fluorescence imaging alone was found insufficient. In addition, preoperative SN mapping also allows the identification of aberrant drainage profiles, which might be missed when only fluorescence imaging is performed.

The intraoperative detection of additional intraoperative SNs is not uncommon, but it is striking that, in our overall study population, 19.3% (59 of 305) additional SNs were intraoperatively identified through the combined use of gamma detection (using a portable gamma camera and gamma probe) and fluorescence imaging. Previous studies from our institute showed that, with the conventional approach (gamma probe and blue dye), next to the preoperatively identified SNs, 8-11.6% additional SNs were harvested [8,29,30]. Because leaving an SN behind constitutes one of the possible causes for false-negative results, this finding indicates that thorough confirmation of SN removal (e.g. by using a portable gamma camera) remains of importance. Retrospective analysis suggests that more careful evaluation of the preoperatively acquired CT and corresponding SPECT images may have helped to better predict the number of preoperative SNs in that area.

While the particle charge was shown not to affect the migratory behavior of tracers in the lymphatic system [31], migration is reversely related to the particle size [32]. Logically, the use of tracers such as ICG (size of ICG <1 nm and 6-7 nm when bound to human serum albumin) or blue dye (<1 nm) may result in the visualization of more nodes compared with the use of large colloidal tracers. For example, through the use of ICG, Fujisawa et al. [11] showed the identification of 24% additional nodes compared with preoperatively identified SNs by using ^{99m}Tc-tin colloid. In addition to their more extensive drainage pattern

compared with large colloidal tracers, the fast drainage of small tracers limits the effective time window in which nodes can be detected through fluorescence imaging. It has been suggested that the optimal time window between injection and visualization of the nodes is 5-30 min [33,34]. For colloidal tracers such as ^{99m}Tc-nanocolloid, retention in the SNs is at least 24 h, thereby allowing both preoperative lymphatic mapping and intraoperative gamma tracing. In our study, in which ICG-^{99m}Tc-nanocolloid was formed via non-covalent self-assembly of ICG and ^{99m}Tc-nanocolloid, we were able to detect the SNs with both gamma tracing and fluorescence imaging up to 27 h after injection. During ex vivo analysis, we did not observe any SNs that were only fluorescent and not radioactive, suggesting the stability of our hybrid tracer over time.

In addition to the difference in nodal retention, there is a clear difference in the optical detection mechanisms for blue dye and near-infrared fluorescence tracers. Blue dye is visible to the eye when it reflects light [35], which is a very superficial effect. On the other hand, the generation of a near-infrared fluorescent signal is an active process in which the fluorescent molecule (in this case ICG) is excited by light of a near-infrared wavelength (±780 nm). Its subsequent relaxation to the ground state results in the emission of light of an even higher wavelength (±820 nm). With the excitation and emission both taking place in the near-infrared window, the near-infrared fluorescence signal can penetrate a tissue layer up to 1.0 cm [36]. However, it must be noted that the signal becomes very diffuse at this depth. The use of ICG facilitates superior in-depth optical identification compared with the use of blue dye; in five patients, near-infrared fluorescence imaging allowed transcutaneous visualization of the SN. In three patients, we could clearly visualize a fluorescent lymphatic duct running to the SN. For future studies, it would be interesting to investigate the hybrid tracer's potential to follow the afferent lymph vessel in comparison with blue dye [32].

Literature has shown that only 0.34-0.92% of the injected tracer is retained per SN; most of the rest of the tracer resides at the injection site [37]. Thus, when an SN is located near the injected melanoma site, radioactivity-based SN identification may be facilitated by removing the site of injection (and thus this unwanted background signal) prior to performing the SN biopsy procedure. Using a hybrid tracer, which combines the fluorescent and radioactive signature in one compound, may improve logistics in daily clinical practice, as no additional injections during the operation are required to allow for optical SN identification (usable in both one- and two-day protocols). This renders the effectiveness of the hybrid approach independent from the order in which the repeat excision of the melanoma site and SN biopsy are performed.

In our study population, most patients (n=69) received both the injection with the hybrid tracer and the injection with the blue dye. This might have led to a bias toward blue dye but not favorable to fluorescence imaging-based SN visualization. Because blue dye is visible to the naked eye, a surgeon cannot be blinded to this factor. However, for visualization of the fluorescent signature of the hybrid tracer, a dedicated fluorescence camera is required, meaning that the surgeon is initially blinded to it. Moreover, during the

operation, surgeons approached the preoperative SNs first with the gamma probe and then blue dye detection. Fluorescence imaging was used last so that its findings could be compared with the findings of the other techniques. In that order It would have been unethical to blind them for these routine technologies. To determine the true value of ICG-^{99m}Tc-nanocolloid (particularly the added value of the hybrid approach) in comparison with the use of a radioactive tracer and blue dye, prospective multicenter randomized studies have to be initiated in which both methods are compared. The potential advantages also need to be weighed against the complexity of the implementation of this hybrid approach into the clinical routine and the associated costs [24]. Fluorescence imaging is rather intuitive and can be used successfully with minimal training. However, the highest additional costs lie in obtaining a near-infrared fluorescence camera system, which, depending on the system chosen (e.g. goggles, handheld, or stand alone), varies from several thousands to hundreds of thousands of U.S. dollars [38]; the list price of the system used in our study is approximately $40,000 in U.S. dollars.

CONCLUSION

ICG-^{99m}Tc-nanocolloid enables both preoperative SN mapping and intraoperative SN identification in patients with melanoma. In our setup, optical identification of the SNs through the fluorescent signature of the hybrid tracer was superior compared with SN identification with blue dye. The fluorescent signature of the hybrid tracer was found to be of additional value for the detection of SNs close to the injection site (two patients), SNs located in an area of complex anatomy (head and neck, 28 patients), and SNs that failed to accumulate blue dye (19 patients).

REFERENCES

1. Valsecchi ME, Silbermins D, de Rosa N, Wong SL, Lyman GH. Lymphatic mapping and sentinel lymph node biopsy in patients with melanoma: a meta-analysis. J Clin Oncol. 2011;29:1479-87.
2. Nieweg OE, Jansen L, Kroon BB. Technique of lymphatic mapping and sentinel node biopsy for melanoma. Eur J Surg Oncol. 1998;24:520-4.
3. Chao C, Wong SL, Edwards MJ, Ross MI, Reintgen DS, Noyes RD, et al. Sentinel lymph node biopsy for head and neck melanomas. Ann Surg Oncol. 2003;10:21-6.
4. Govaert GA, Oostenbroek RJ, Plaisier PW. Prolonged skin staining after intradermal use of patent blue in sentinel lymph node biopsy for breast cancer. Eur J Surg Oncol. 2005;31:373-5.
5. Nieweg OE, Veenstra HJ. False-negative sentinel node biopsy in melanoma. J Surg Oncol. 2011;104:709-10.

6. van Akkooi AC, Voit CA, Verhoef C, Eggermont AM. New developments in sentinel node staging in melanoma: controversies and alternatives. Curr Opin Oncol. 2010;22:169-77.
7. Uren RF. SPECT/CT Lymphoscintigraphy to locate the sentinel lymph node in patients with melanoma. Ann Surg Oncol. 2009;16:1459-60.
8. Veenstra HJ, Vermeeren L, Olmos RA, Nieweg OE. The additional value of lymphatic mapping with routine SPECT/CT in unselected patients with clinically localized melanoma. Ann Surg Oncol. 2012;19:1018-23.
9. Vermeeren L, Valdes Olmos RA, Klop WM, van der Ploeg IM, Nieweg OE, Balm AJ, et al. SPECT/CT for sentinel lymph node mapping in head and neck melanoma. Head Neck. 2011;33:1-6.
10. Vermeeren L, Valdes Olmos RA, Klop WM, Balm AJ, van den Brekel MW. A portable gamma-camera for intraoperative detection of sentinel nodes in the head and neck region. J Nucl Med. 2010;51:700-3.
11. Fujisawa Y, Nakamura Y, Kawachi Y, Otsuka F. Indocyanine green fluorescence-navigated sentinel node biopsy showed higher sensitivity than the radioisotope or blue dye method, which may help to reduce false-negative cases in skin cancer. J Surg Oncol. 2012;106:41-5.
12. Gilmore DM, Khullar OV, Gioux S, Stockdale A, Frangioni JV, Colson YL, et al. Effective low-dose escalation of indocyanine green for near-infrared fluorescent sentinel lymph node mapping in melanoma. Ann Surg Oncol. 2013;20:2357-63.
13. Nakamura Y, Fujisawa Y, Nakamura Y, Maruyama H, Furuta J, Kawachi Y, et al. Improvement of the sentinel lymph node detection rate of cervical sentinel lymph node biopsy using real-time fluorescence navigation with indocyanine green in head and neck skin cancer. J Dermatol. 2013 Jun;40:453-7.
14. Namikawa K, Tsutsumida A, Tanaka R, Kato J, Yamazaki N. Limitation of indocyanine green fluorescence in identifying sentinel lymph node prior to skin incision in cutaneous melanoma. Int J Clin Oncol. 2014;19:190-203.
15. Stoffels I, von der Stuck H, Boy C, Poppel T, Korber N, Weindorf M, et al. Indocyanine green fluorescence-guided sentinel lymph node biopsy in dermato-oncology. J Dtsch Dermatol Ges. 2012 Jan;10:51-7.
16. van der Vorst JR, Schaafsma BE, Verbeek FP, Swijnenburg RJ, Hutteman M, Liefers GJ, et al. Dose optimization for near-infrared fluorescence sentinel lymph node mapping in patients with melanoma. Br J Dermatol. 2013;168:93-8.
17. van Leeuwen AC, Buckle T, Bendle G, Vermeeren L, Valdes Olmos R, van de Poel HG, et al. Tracer-cocktail injections for combined pre- and intraoperative multimodal imaging of lymph nodes in a spontaneous mouse prostate tumor model. J Biomed Opt. 2011;16:016004.
18. Buckle T, van Leeuwen AC, Chin PT, Janssen H, Muller SH, Jonkers J, et al. A self-assembled multimodal complex for combined pre- and intraoperative imaging of the sentinel lymph node. Nanotechnology. 2010;21:355101.

19. Brouwer OR, Buckle T, Vermeeren L, Klop WM, Balm AJ, van der Poel HG, et al. Comparing the hybrid fluorescent-radioactive tracer indocyanine green-^{99m}Tc-nanocolloid with ^{99m}Tc-nanocolloid for sentinel node identification: a validation study using lymphoscintigraphy and SPECT/CT. J Nucl Med. 2012;53:1034-40.
20. Brouwer OR, van den Berg NS, Matheron HM, van der Poel HG, van Rhijn BW, Bex A, et al. A hybrid radioactive and fluorescent tracer for sentinel node biopsy in penile carcinoma as a potential replacement for blue dye. Eur Urol. 2014;65:600-9.
21. Brouwer OR, Klop WM, Buckle T, Vermeeren L, van den Brekel MW, Balm AJ, et al. Feasibility of sentinel node biopsy in head and neck melanoma using a hybrid radioactive and fluorescent tracer. Ann Surg Oncol. 2012;19:1988-94.
22. Mathéron HM, van den Berg NS, Brouwer OR, Kleinjan GH, van Driel WJ, Trum JW, et al. Multimodal surgical guidance towards the sentinel node in vulvar cancer. Gynecol Oncol. 2013;131:720-5
23. Schaafsma BE, Verbeek FP, Rietbergen DD, van der Hiel B, van der Vorst JR, Liefers GJ, et al. Clinical trial of combined radio- and fluorescence-guided sentinel lymph node biopsy in breast cancer. Br J Surgery. 2013;100:1037-44.
24. van den Berg NS, Brouwer OR, Klop WM, Karakullukcu B, Zuur CL, Tan IB, et al. Concomitant radio- and fluorescence-guided sentinel lymph node biopsy in squamous cell carcinoma of the oral cavity using ICG-(^{99m})Tc-nanocolloid. Eur J Nucl Med Mol Imaging. 2012;39:1128-36.
25. van der Poel HG, Buckle T, Brouwer OR, Valdes Olmos RA, van Leeuwen FW. Intraoperative laparoscopic fluorescence guidance to the sentinel lymph node in prostate cancer patients: clinical proof of concept of an integrated functional imaging approach using a multimodal tracer. Eur Urol. 2011;60:826-33.
26. Bunschoten A, Buckle T, Kuil J, Luker GD, Luker KE, Nieweg OE, et al. Targeted non-covalent self-assembled nanoparticles based on human serum albumin. Biomaterials. 2012;33:867-75.
27. Nieweg OE, Tanis PJ, Kroon BB. The definition of a sentinel node. Ann Surg Oncol. 2001;8:538-41.
28. Valdés Olmos RA, Vidal-Sicart S. SPECT/CT image generation and criteria for sentinel node mapping. In: Mariani G., Manca G, Orsini P., Vidal-Sicart S., Valdés Olmos R., eds. Atlas of Lymphoscintigraphy and Sentinel Node Mapping. Milan, Italy: Springer; 2012. p. 269-83.
29. Klop WM, Veenstra HJ, Vermeeren L, Nieweg OE, Balm AJ, Lohuis PJ. Assessment of lymphatic drainage patterns and implications for the extent of neck dissection in head and neck melanoma patients. J Surg Oncol. 2011;103:756-60.
30. Veenstra HJ, Klop WM, Speijers MJ, Lohuis PJ, Nieweg OE, Hoekstra HJ, et al. Lymphatic drainage patterns from melanomas on the shoulder or upper trunk to cervical lymph nodes and implications for the extent of neck dissection. Ann Surg Oncol. 2012;19:3906-12.

31. Ballou B, Lagerholm BC, Ernst LA, Bruchez MP, Waggoner AS. Noninvasive imaging of quantum dots in mice. Bioconjug Chem. 2004;15:79-86.
32. Uren RF. Lymphatic drainage of the skin. Ann Surg Oncol. 2004;11:179S-85S.
33. Bredell MG. Sentinel lymph node mapping by indocyanin green fluorescence imaging in oropharyngeal cancer - preliminary experience. Head Neck Oncol. 2010;2:31.
34. Jeschke S, Lusuardi L, Myatt A, Hruby S, Pirich C, Janetschek G. Visualisation of the lymph node pathway in real time by laparoscopic radioisotope- and fluorescence-guided sentinel lymph node dissection in prostate cancer staging. Urology. 2012;80:1080-6.
35. van den Berg NS, van Leeuwen FW, van der Poel HG. Fluorescence guidance in urologic surgery. Curr Opin Urol. 2012;22:109-20.
36. Vahrmeijer AL, Frangioni JV. Seeing the invisible during surgery. Br J Surg. 2011;98:749-50.
37. Mariani G, Erba P, Manca G, Villa G, Gipponi M, Boni G, et al. Radioguided sentinel lymph node biopsy in patients with malignant cutaneous melanoma: the nuclear medicine contribution. J Surg Oncol. 2004;85:141-51.
38. Liu Y, Bauer AQ, Akers WJ, Sudlow G, Liang K, Shen D, et al. Hands-free, wireless goggles for near-infrared fluorescence and real-time image-guided surgery. Surgery. 2011;149:689-98.

SUPPORTING INFORMATION

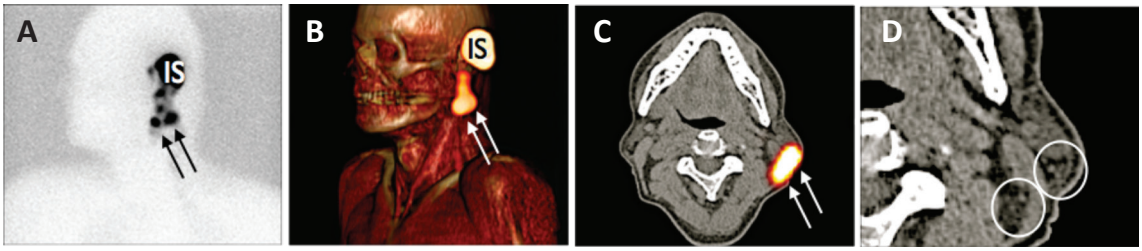

Figure SI1. Preoperative sentinel node mapping in a 59-year-old male patient with head-and-neck melanoma (left ear; Breslow thickness 1.0 mm). The patient was scheduled for re-excision of the melanoma scar and subsequent SN biopsy. Due to the location of the melanoma, no patent blue dye was injected intraoperatively. Conventional lymphoscintigrams (A) and SPECT/CT images (B) showing SNs in the parotid gland and level II (marked with arrows). Intraoperatively, additional SNs were from both locations. Retrospective analysis revealed the SNs in the parotid gland and level II being part of clusters (four and two nodes harvested, respectively; C and D) SN = sentinel node; IS = injection site; SPECT/CT = single photon emission computed tomography combined with computed tomography.

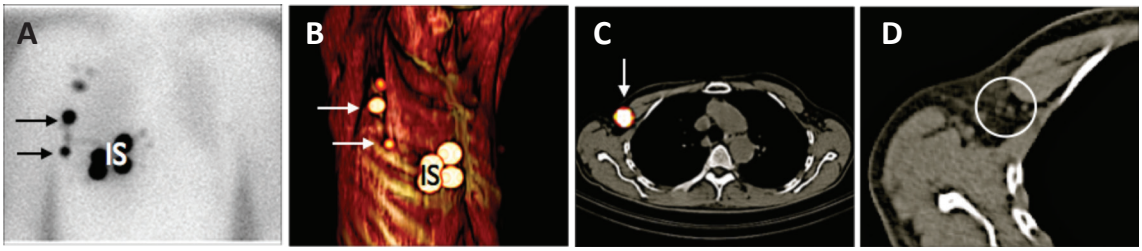

Figure SI2. Preoperative sentinel node mapping in 69-year-old male patient with a melanoma of the trunk (thorax right; Breslow thickness 4.0 mm). The patient was scheduled for re-excision of the melanoma scar and subsequent SN biopsy. Directly before the start of the operation 1.0 mL patent blue dye was injected. Conventional lymphoscintigrams (A) and SPECT/CT. images (B) showing two SNs (pectoral and axilla; marked with arrows) with regard to the injection site (IS). Intraoperatively, four SNs were removed from the axilla. Retrospective analysis revealed these SNs being part of a cluster (C and D). SN = sentinel node; IS = injection site; SPECT/CT = single photon emission computed tomography combined with computed tomography.

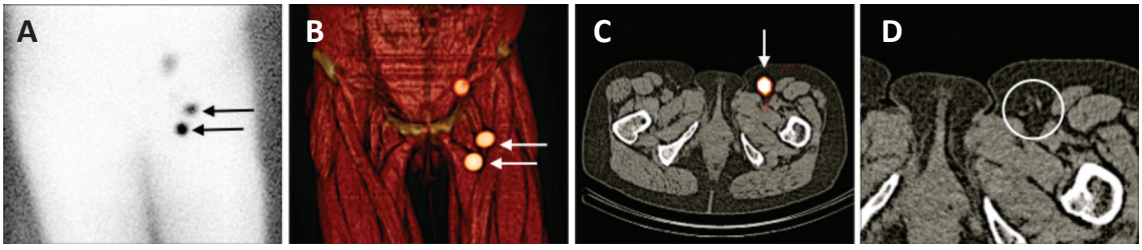

Figure SI3. Preoperative sentinel node mapping in a 65-year-old female patient with melanoma of an extreemity (left medial knee; Breslow thickness 2.1 mm). The patient was scheduled for re-excision of the melanoma scar and subsequent SN biopsy. Directly before the start of the operation 1.0 mL patent blue dye was injected. Conventional lymphoscintigrams (A) and SPECT/CT images (B) showing two SNs in the groin (marked with arrows) with regard to the injection site (IS). Intraoperatively, three SNs were removed from the groin. Retrospective analysis revealed these SNs being part of a cluster (C and D). SN = sentinel node; IS = injection site; SPECT/CT = single photon emission computed tomography combined with computed tomography.